Atomic N-shell Coster-Kronig, Auger, and radiative rates and fluorescence yields for $38 \leq Z \leq 103$†

Eugene J. McGuire
Sandia Laboratories, Albuquerque, New Mexico 87115

(Received 7 January 1974)

Calculated N-shell Auger and radiative transition rates, yields, and level widths for $38 \leq Z \leq 103$ were reported. To calculate the $N_{6,7}$ transition rates it was necessary to find formal expressions in LS coupling for the Auger transition rate with initial f holes. In so doing it was found that some expressions previously given for Auger transition rates involving initial f holes were in error. The corrected expressions are presented herein. Because there exist no data on N-shell fluorescence yields, all comparisons with experiment are comparisons of level widths obtained in most instances from x-ray linewidth measurements. For $Z \leq 57$ the calculated values are in reasonable agreement with experiment. However, when the $4f$ shell begins to be filled the calculated N-shell level widths appear to be significantly larger than the experimental level widths. Some of the discrepancy can be attributed to the sensitivity to Auger-electron energy of the $(4l)$-$(4l')(4f)$ super-Coster-Kronig-process.

I. INTRODUCTION

Calculations of Auger transition rates and fluorescence yields have been done for the K,[1-3] L,[4-6] and M shells.[7,8] There are extensive measurements on K-shell fluorescence yields, considerably fewer on the L shell, and a small number on the M shell. There are none on the N shell. Consequently comparisons between N shell yield calculations and experiment are limited to comparisons of widths. There is one measurement of N-shell Auger electron spectra, the $N_{4,5}OO$ spectrum of Xe.[9] We plan to discuss it in a later paper on N-shell electron spectra.[10] Measurements of N-shell widths can be found from K- and L-shell hard-x-ray emission spectra,[11-17] M- and N-shell soft-x-ray emission spectra,[18-21] and N-shell photoelectron spectroscopy.[22] Some of the N-shell data were obtained to examine multiplet splitting in ions with partially filled N subshells. In such cases the multiplet splitting is an additional factor that must be accounted for in determining a measured width. We have treated this elsewhere.[23] For $Z > 57$, decay of $4s$, $4p$, and $4d$ vacancies is dominated by Coster-Kronig and super-Coster-Kronig[7]-transitions involving $4f$ electrons. In addition $4f$ vacancies can decay by Auger transitions and it was necessary to determine expressions for the Auger transition for initial f holes. In so doing it was discovered that expressions given earlier[24] by the author for the Auger transition rate for initial s and $\bar{p}$ holes and f electrons contain errors. The corrected values are given in Sec. II. Because of the complexity of the Auger transition rates for initial f holes calculated in j-j coupling, the transition rates were calculated in LS coupling only. This precludes any calculation of Coster-Kronig transitions of the form N_6-N_7X.

II. TRANSITION RATES, ENERGETICS, AND ORBITALS

Expressions for the Auger transition rates in LS coupling for initial f holes are given in the Appendix. If the Auger transition rate for an ion whose initial state has an l_1 hole, and whose final state has l_3 and l_4 holes and an l_2 electron in the continuum, is written $W(l_1 l_2 l_3 l_4)$ then $W(l_1 l_2 l_3 l_4) = [(2l_1+1)/2l_3+1]W(l_3 l_4 l_1 l_2)$. Thus one can compare transition rate expressions for initial f holes, with expressions involving final-state f holes. In comparing the results in the Appendix with those earlier found by the author, several errors in Ref. 24 were discovered. For transitions s-ff' the Auger transition rate is

$$\begin{aligned} W_{if}(s, ff') = {} & 2\pi \times 14\tau^2 \{D(3,0)^2 + E(3,0)^2 - D(3,0)E(3,0) \\ & + \tfrac{4}{3}[D(3,2)^2 + E(3,2)^2 - D(3,2)E(3,2)] \\ & + \tfrac{8}{11}[D(3,4)^2 + E(3,4)^2 - D(3,4)E(3,4)] \\ & + \tfrac{100}{33}[D(3,6)^2 + E(3,6)^2 - D(3,6)E(3,6)]\}, \end{aligned} \tag{1}$$

where $D(K, l)$, $E(K, l)$, and τ^2 are defined in the Appendix. In addition in Ref. 24 the expression for the $\bar{p}$-ff transition contains the terms $+\frac{54}{35}D(2,1)E(2,1) + \cdots + \frac{12}{11}D(4,3)E(4,3)$. The corrected terms are $-\frac{18}{35}D(2,1)E(2,1) + \cdots - \frac{24}{11}D(4,3)$

$\times E(4,3)$. With these exceptions the expressions given in the Appendix are consistent with those in Ref. 24. Since $3s$-$(4f)^2$ and $3p$-$(4f)^2$ transitions are weak, the above-mentioned errors have no significant effect on earlier work. It has been pointed out to the author[25] that three other errors occur in Ref. 24. The expression for the $\bar{d}$-$\bar{d}\bar{d}$ Auger transition rate contains a term $4(A_2+D_2)$ which should be $4(A_2+C_2)$, and that the coefficients of $D(4,4)$ and $E(4,4)$ in the expressions for B_2 and D_2, respectively, should be $\frac{20}{77}$ instead of $\frac{20}{7}$. These errors are not negligible and led to calculated $3d$ widths[7] that were as much as ten percent too large. The Auger transition rate calculations reported here used the j-j coupling expressions given by Asaad[26] and by the author,[24] and the LS coupling results listed in the Appendix.

The decay of N-shell holes is dominated by Coster-Kronig transitions of the form N-NX and super-Coster-Kronig-transitions of the form N-NN. In such transitions a low-energy electron is ejected from the ion. The computed transition rate is sensitive to the choice of ejected electron energy, and there are few measurements of the energy of the ejected electron. In these calculations the energy of the ejected electron was estimated using

$$\epsilon = E_{n_1 l_1}(Z) - \tfrac{1}{2}[E_{n_3 l_3}(Z) + E_{n_3 l_3}(Z+1) + E_{n_4 l_4}(Z) + E_{n_4 l_4}(Z+1)], \quad (2)$$

where $E_{nl}(Z)$ is the binding energy for the nl subshell of the neutral atom with nuclear charge Z. Red'kin *et al.*[27] have measured the low-energy Auger electron spectrum of osmium ($Z=76$), exciting inner-shell vacancies with 1.0–0.4-keV electrons. The observed spectra were independent of the exciting electron energy in the energy range studied. They observed three peaks at 158, 163, and 172 eV, and peaks at 9 and 21 eV. They assign the high-energy peaks to N_5-$N_{6,7}N_{6,7}$ transitions. Using Eq. (2) and the electron spectroscopy for chemical analysis (ESCA) tabulation of[28] binding energies we find $\epsilon = 161$ eV, in good agreement with the measurements. For N_2-N_3O_2 and N_2-N_3O_3 transitions Eq. (2) leads to +5 and +17 eV, respectively, in agreement with the measured values of +9 and +21 eV. Our calculations indicate that N_4-$N_{6,7}N_{6,7}$ transitions are comparable in strength to N_5-$N_{6,7}N_{6,7}$ transitions and occur at $\epsilon = 174$ eV. The ESCA tabulation of binding energies shows at N_6-N_7 splitting of 2–3 eV near $Z=76$. Thus it appears the structure seen by Red'kin *et al.* between 158 and 172 eV should be assigned to $N_{4,5}$-$N_{6,7}N_{6,7}$ transitions, not merely to N_5-$N_{6,7}N_{6,7}$ transitions.

As in previous work,[1,4,7] I determined the discrete and continuum orbitals by approximating the central potential of Herman and Skillman[29] for an ion with a $4p$ hole by a series of seven straight lines, varying the parameters of the approximation until the eigenvalues are in reasonable agreement with the eigenvalues of Herman and Skillman.[30] The bound and continuum orbitals are then obtained in terms of Whittaker functions. For $Z=96$, 100, and 103 the ESCA tabulation[28] of binding energies has no entries for $N_{6,7}$, O, and P shells. For these cases we used the model eigenvalues in determining the Auger-electron energy.

III. CALCULATED YIELDS

In Table I we list the calculated N_1 yields for $38 \leq Z \leq 103$; in Table II we list the N_2 and N_3 yields for $38 \leq Z \leq 103$; and in Table III we list the N_4 and N_5 yields for $50 \leq Z \leq 103$, and the $N_{6,7}$ fluorescence yields and level widths for $70 \leq Z \leq 103$. The fluorescence yield ω_i^N is the ratio of the total radiative decay rate to the total decay rate. The Auger yield a_i^N is the ratio of the total decay rate via N_i-XY transitions, where $X, Y \neq N$, to the total decay rate. Because of the occurrence of super-Coster-Kronig-transitions of the form N_i-N_jN_k, the first step in the decay of an N_i vacancy can lead to two other N vacancies. The quantity $S(N_i, N_j)$ is the average number of N_j vacancies produced in the first step of the decay of an N_i vacancy. We emphasize the first step because it is possible for several $N_{6,7}$ vacancies to be created in the decay of an N_1 vacancy. In general,

$$\omega_i^N + a_i^N + \sum_j S(N_i, N_j) \leq 2, \quad (3a)$$

and when super-Coster-Kronig-transitions are forbidden,

$$\omega_i^N + a_i^N + \sum S(N_i, N_j) = 1. \quad (3b)$$

The total transition rate is listed in terms of widths Γ. The total transtion rate is $\Gamma/\hbar$.

The $N_{6,7}$ widths are less than 1 eV for all the elements up to $Z=100$. This is due to the absence of Coster-Kronig transitions. The N_4 and N_5 widths are less than 1 eV until the $4f$ shell begins being filled. The ESCA tabulation of binding energies does not list a splitting of the N_4 and N_5 binding energies until $Z=70$. For $Z \geq 73$ the N_4-N_5 splitting is less than the $N_{6,7}$ binding energy, and for $Z \geq 73$ we neglected N_4-$N_5N_{6,7}$ transitions. For $Z=70$ the listed N_4-N_5 splitting is greater than the $N_{6,7}$ binding energy and the N_4-$N_5N_{6,7}$ transition rate is large. The possibility exists for N_4-$N_5N_{6,7}$ transitions in the other rare earths but,

TABLE I. Calculated N_1 yields and widths (in eV) for $38 \leq Z \leq 103$. The width values in parentheses are obtained using an alternate Auger-electron energy estimate as discussed in the text. The notation A-B is $A \times 10^{-B}$.

		N_1 yields							
Z	ω_1^N	$S(1,2)$	$S(1,3)$	$S(1,4)$	$S(1,5)$	$S(1,67)$	$\mathfrak{A}_1^N$	Γ(eV)	
38	1.2-5	0.33	0.66	···	···	···	0.017	0.70	
40	2.1-6	0.31	0.63	0.36	0.53	···	0.0017	6.44	(6.2)
42	1.3-6	0.33	0.66	0.40	0.59	···	···	14.8	(8.0)
44	1.1-6	0.32	0.65	0.41	0.61	···	···	22.9	(8.0)
47	8.0-7	0.32	0.64	0.41	0.62	···	···	41.9	(7.0)
50	6 2-7	0.33	0.65	0.40	0.60	···	0.0003	78.2	(3.1)
54	1.5-5	0.20	0.40	0.23	0.35	···	0.014	5.49	
57	2.3-5	0.22	0.43	0.20	0.30	···	0.017	6.87	
58	2.2-5	0.23	0.47	0.15	0.23	0.17	0.012	8.28	
60	2.2-5	0.24	0.48	0.14	0.21	0.38	0.011	10.0	
63	2.8-5	0.25	0.50	0.11	0.16	0.48	0.007	11.4	
65	3.3-5	0.25	0.49	0.11	0.16	0.59	0.008	12.6	
67	3.7-5	0.25	0.50	0.10	0.15	0.64	0.006	14.8	
70	4.9-5	0.25	0.50	0.080	0.12	0.65	0.005	15.1	
73	6.1-5	0.20	0.56	0.073	0.11	0.63	0.007	16.3	
74	7.5-5	0.19	0.56	0.062	0.092	0.59	0.008	15.0	
77	1.0-4	0.19	0.57	0.059	0.091	0.56	0.013	16.0	
79	1.3-4	0.27	0.50	0.049	0.074	0.45	0.013	15.9	
83	2.4-4	0.26	0.46	0.055	0.083	0.38	0.021	14.1	
86	3.6-4	0.22	0.47	0.053	0.080	0.41	0.026	12.3	
90	6.1-4	0.31	0.33	0.059	0.088	0.27	0.034	11.2	
92	7.1-4	0.36	0.33	0.049	0.074	0.25	0.029	11.8	
96	8.3-4	0.42	0.25	0.051	0.077	0.23	0.040	14.0	
100	0.0012	0.53	0.18	0.048	0.072	0.19	0.036	15.3	
103	0.0016	0.46	0.20	0.048	0.073	0.24	0.040	14.7	

TABLE II. Calculated N_2 and N_3 yields and widths (in eV) for $38 \leq Z \leq 103$.

	N_3 yields						N_2 yields						
Z	ω_3^N	$S(3,4)$	$S(3,5)$	$S(3,67)$	$\mathfrak{A}_3^N$	Γ(eV)	ω_2^N	$S(2,3)$	$S(2,4)$	$S(2,5)$	$S(2,67)$	$\mathfrak{A}_4^N$	Γ(eV)
38	0.013	···	···	···	1.0	6×10^{-5}	0.013	···	···	···	···	1.0	6×10^{-5}
40	2.3-5	0.52	1.25	···	0.0006	0.27	2.3-5	···	1.08	0.69	···	0.0006	0.27
42	7.2-6	0.62	1.35	···	···	2.03	7.2-6	···	1.12	0.85	···	···	2.03
44	6.2-6	0.63	1.36	···	···	4.82	6.2-6	···	1.12	0.86	···	···	4.82
47	8.4-6	0.63	1.36	···	···	9.69	8.4-6	···	1.12	0.87	···	···	9.69
50	7.0-6	0.62	1.34	···	0.0007	16 2	7.0-6	···	1.11	0.85	···	0.0007	16.2
54	5.5-5	0.20	0.77	···	0.03	2.56	5.5-5	···	0.76	0.21	···	0.029	2.56
57	8.5-5	0.21	0.745	···	0.045	2.72	1.1-4	0.018	0.73	0.21	···	0.042	2.83
58	5.9-5	0.18	0.76	0.41	0.023	3.90	8.1-5	0.061	0.72	0.16	0.44	0.022	4.15
60	5.6-5	0.17	0.75	0.57	0.018	5.48	7.3-5	0.065	0.72	0.15	0.59	0.017	5.86
63	5.6-5	0.16	0.76	0.71	0.012	7.14	7.2-5	0.134	0.68	0.11	0.70	0.011	8.25
65	5.6-5	0.16	0.75	0.77	0.011	8.80	7.0-5	0.127	0.68	0.11	0.75	0.009	10.1
67	5.9-5	0.15	0.76	0.80	0.009	9.86	7.0-5	0.142	0.67	0.10	0.81	0.008	11.2
70	5.2-5	0.14	0.75	0.86	0.007	12.1	6.5-5	0.122	0.69	0.10	0.84	0.006	13.7
73	5.9-5	0.15	0.74	0.87	0.009	12 9	7.5-5	0.118	0.68	0.10	0.84	0.008	14.6
74	6.9-5	0.14	0.73	0.82	0.011	12.3	8.0-5	0.114	0.67	0.10	0.79	0.010	13.8
77	7.7-5	0.15	0.74	0.80	0.012	12.8	1.0-4	0.119	0.68	0.10	0.77	0.011	14.5
79	9.0-5	0.14	0.71	0.74	0.017	12.9	1.2-4	0.090	0.67	0.10	0.68	0.016	14.2
83	1.4-4	0.14	0.65	0.62	0.033	11.9	1.9-4	0.144	0.58	0.10	0.53	0.028	13.9
86	1.2-4	0.14	0.72	0.66	0.021	16.3	2.0-4	0.047	0.72	0.11	0.63	0.020	17.1
90	4.5-4	0.13	0.57	0.34	0.054	7.49	6.7-4	0.092	0.53	0.11	0.30	0.048	8.27
92	5.9-4	0.13	0.55	0.29	0.062	6.63	9.0-4	0.111	0.49	0.11	0.26	0.055	7.46
96	6.9-4	0.13	0.55	0.25	0.080	7.59	1.05-3	0.113	0.50	0.10	0.22	0.071	8.54
100	1.03-3	0.12	0.49	0.31	0.092	7.20	1.6-3	0.183	0.39	0.10	0.25	0.075	8.81
103	1.32-3	0.12	0.48	0.32	0.103	6.96	2.2-3	0.174	0.40	0.10	0.25	0.085	8.44

TABLE III. Calculated N_4, N_5, and $N_{6,7}$ yields and widths (in eV) for $38 \leq Z \leq 103$.

	N_4 yields					N_5 yields				N_6 yields	
Z	ω_4^N	$S(4,5)$	$S(4,67)$	$\mathfrak{A}_4^N$	Γ(eV)	ω_5^N	$S(5,67)$	$\mathfrak{A}_5^N$	Γ(eV)	ω_{67}^N	Γ(eV)
50	4.2-6	···	···	1.0	0.14	4.2-6	···	1.0	0.14	···	···
54	6.3-5	···	···	1.0	0.082	6.3-5	···	1.0	0.082	···	···
57	1.4-4	···	···	1.0	0.133	1.4-4	···	1.0	0.133	···	···
58	1.9-4	···	1.02	0.20	0.34	1.9-4	1.02	0.20	0.339	···	···
60	1.3-4	···	1.40	0.080	0.89	1.3-4	1.40	0.080	0.892	···	···
63	1.1-4	···	1.62	0.029	2.07	1.1-4	1.67	0.029	2.07	···	···
65	1.1-4	···	1.72	0.015	3.16	1.1-4	1.72	0.015	3.16	···	···
67	1.1-4	···	1.75	0.016	4.34	1.1-4	1.75	0.016	4.34	···	···
70	0.7-4	0.45	1.41	0.004	9.35	0.9-4	1.82	0.005	7.24	0.0	2.-4
73	1.2-4	0.015	1.74	0.012	7.73	1.2-4	1.77	0.012	7.61	3.6-6	0.053
74	1.2-4	0.021	1.70	0.012	7.89	1.3-4	1.73	0.013	7.72	7.2-6	0.070
77	1.3-4	0.034	1.61	0.024	8.63	1.4-4	1.80	0.027	8.34	2.1-5	0.154
79	1.5-4	0.049	1.51	0.032	8.83	1.6-4	1.59	0.033	8.40	3.9-5	0.232
83	2.3-4	0.003	1.63	0.048	7.56	2.3-4	1.63	0.048	7.54	1.8-4	0.128
86	2.8-4	0.004	1.07	0.056	7.02	2.8-4	1.07	0.057	6.99	4.4-4	0.098
90	4.7-4	0.002	1.02	0.094	5.27	4.7-4	1.02	0.094	5.25	4.6-4	0.152
92	7.0-4	0.016	0.871	0.113	4.23	7.2-4	0.886	0.114	4.17	3.1-4	0.288
96	7.9-4	0.021	0.849	0.130	5.36	8.1-4	0.868	0.132	5.25	2.5-4	0.571
100	1.2-3	0.032	0.813	0 153	5.86	1.2-3	0.841	0.158	5.68	2.9-4	0.876
103	1.3-3	0.030	0.832	0.138	6.66	1.4-3	0.857	0.142	6.46	2.9-4	1.12

in the absence of data on the N_4-N_5 splitting we neglected such transitions at $Z=63$, 65, and 67. For $40 \leq Z \leq 50$ the N_2 and N_3 widths are dominated by $N_{2,3}$-$N_{4,5}N_{4,5}$ super-Coster-Kronig-transitions. Again, in the absence of data on the N_2-N_3 splitting we neglected N_2-$N_3N_{4,5}$ transitions. For $50 < Z \leq 57$ the dominant transitions are $N_{2,3}$-$N_{4,5}O$, and above $Z=58$ Coster-Kronig transitions involving $4f$ electrons are dominant in determining the N_2 and N_3 widths. The N_1 widths follow a pattern similar to the $N_{2,3}$ widths, except that for $Z \leq 50$ super-Coster-Kronig-transitions of the form N_1-$N_{2,3}N_{4,5}$ lead to enormous widths, 42 eV for Ag and 78 eV for Sn. The reality of such enormous widths is discussed in Sec. IV.

IV. COMPARISON WITH EXPERIMENT

In comparing the calculations with experiments we take four segments of Z; $38 \leq Z \leq 50$, where the $4d$ shell is being filled; $54 \leq Z \leq 57$; $58 \leq Z \leq 70$, where the $4f$ shell is being filled; and $Z \geq 73$.

a. $38 \leq Z \leq 50$. In the region $38 \leq Z \leq 50$ early work in soft x-ray spectroscopy[31] was concerned with energy levels, and no width measurements are reported. Parratt's study[12] of the L-shell emission spectrum of Ag provides a complete set of L, M, and N subshell widths. The recent measurements of Krause, Wuilleumier, and Nestor[11] on the L-emission spectrum of Zr is the only other study of many level widths in a single element. The width of the L_1-$N_{2,3}$ emission line for $41 \leq Z \leq 50$ has recently been studied by Estig and Källne.[32] The widths of the M_5-N_3 line in a number of elements between $Z=38$ and 47 have been studied by Lukirskii and Zimkina,[19] Dannhäuser and Wiech,[20] and Krause.[21] The measured widths are in essential agreement. In Fig. 1 we have connected with a solid line our N_3 widths calculated at $Z=40$, 42, 44, and 47–50. From the experimental M_5-N_3 widths of Dannhäuser and Wiech[20] we subtracted the M_5 widths of the author[7] to obtain the open circles in Fig. 1. From the measurements of Estig and Källne[32] at $Z=47$–50, we have subtracted a calculated L_1 width[33] (essentially 3 eV in each instance) and obtained the open squares in Fig. 1.

At $Z=47$ both experimental width determinations and the calculated value are in excellent agreement. At $Z=50$ the calculated and measured N_3 widths are in good agreement. They differ, however, at $Z=48$ and 49. The widths are dominated by N_3-$N_{4,5}N_{4,5}$ super-Coster-Kronig-transitions, and the increase in width between $Z=47$ and 50 is due to the contraction of the $4d$ orbital and not to the additional O-shell electrons. The difference between calculated and measured N_3 widths at $Z=48$ and 49 could be due to inaccuracy in the $4d$ orbital used in the calculation or to the estimate of Auger electron energy.

In a study of the effect of multiplet-splitting on Auger transition rates we[23] examined the variation of N_3 widths with Auger electron energy. For the *N_3 shell we found the widths increased as the Auger electron energy decreased.* In comparing the estimate in Eq. (2) with the energy difference found

from spectroscopic data,[34] for cases in which the necessary spectroscopic data are available in Moore's tables,[34] we find Eq. (2) consistently overestimates the energy of the Auger electron by 10-15 eV. Using the spectroscopic data to determine the energy of the final state and the ESCA binding energy tabulation to determine the energy of the initial state, leads to widths substantially larger than those shown in Fig. 1. However, for $Z=42$, 44, and 45, the widths calculated with Auger electron energies from Eq. (2) are larger than the measured values. Lower values of Auger electron energy would increase the disagreement.

There are at least two possible explanations for this. First there is the possibility of multiplet effects. A $4p$ hole added to a partially filled $4d$ shell produces six final-state terms in the $M_{4,5}$-$N_{2,3}$ radiation process. Characteristically in a $4p$-$(4d)^2$ transition the high-spin final-state term has a smaller transition rate and smaller width than the low-spin term. In fact, for the $4d$ shell half-filled or less than half-filled the Auger transition rate is zero.[23] Multiplet splitting has been used in an attempt to account for the $K\beta$ satellite structure seen in the first transition series.[35] The calculations in Ref. 35 are in qualitative but not quantitative agreement with the measurements. A second explanation for the difference between calculated and measured N_3 widths at $Z=42$, 44, and 45 might lie in the approach to bonding in solids advanced by Brewer.[36] Brewer correlates a body-centered cubic structure with a $(4d)^{n-1}(5s)$ configuration, hexagonal closed packed with a $(4d)^{n-2}(5s)(5p)$ configuration, and cubic close packed with $(4d)^{n-3}(5s)(5p)^2$ configurations. The structure of the solid is correlated with the number of valence electrons, as is the number of d electrons available for a $4p$-$(4d)^2$ Auger transition. Our calculations were done assuming a $(4d)^{n-1}$ $5s$ configuration. The dashed line in Fig. 1 was obtained by shifting the solid line by one or two units in Z, depending on the solid-state structure, i.e., hexagonal close packed at $Z=43$ and 44, and cubic close packed at $Z=45$–47.[36] The resultant curve is closer to experiment at $Z=44$ and 45, but is too low by 3 eV at $Z=47$. If the disagreement between theory and experiment is due to solid-state structure then an observation of the $M_{4,5}$-$N_{2,3}$ radiative transition in a free atom should indicate a width twice as large as in the solid at $Z=44$ and 45.

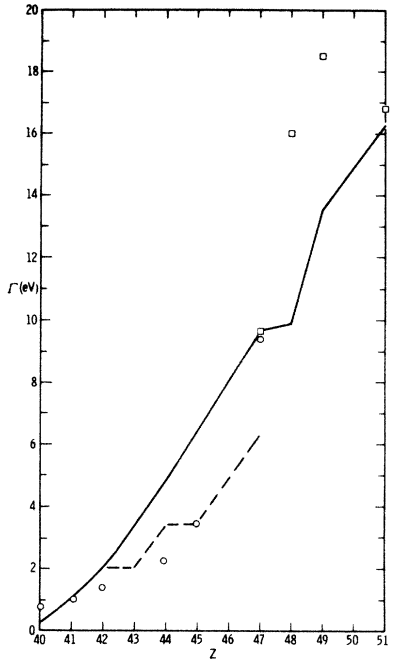

FIG. 1. Calculated and experimental $4p$ level widths for $40 \leq Z \leq 50$. The extraction of experimental level widths from experimental linewidths is discussed in the text. The open circles are from Ref. 20 and the open squares from Ref. 32. The dashed line results from reducing the number of $4d$ electrons in the Auger transition rate as discussed in the text.

From the L_1-$N_{2,3}$ width measurements of Estig and Källne[32] and the N_3 width derived from the measured $M_{4,5}$-$N_{2,3}$ transition one finds $\Gamma_{L_1}=5.5$ at $Z=41$ and $\Gamma_{L_1}=5.9$ at $Z=42$. These values are lower than the values calculated by the author,[4] 8.3 eV at $Z=40$ and 8.1 eV at $Z=42$. Crasemann, Chen, and Kostroun[5] calculate 7.9 eV at $Z=40$ and 6.5 eV at $Z=42$. The difference can be accounted for by the inclusion in the calculations of the L_1-$L_2M_{4,5}$ process, which is probably forbidden by energetics at $Z=40$ and 42 and contributed 1.0 eV to the author's calculated widths, and the sensitivity of the L_1-$L_3M_{4,5}$ transition rate to the estimate of Auger electron energy.

In Table IV we compare the estimates of level widths of Krause, Wuilleumier, and Nestor for Zr ($Z=40$)[11] and Parratt for Ag ($Z=47$)[12] with calculated values. We have determined the M- and N-shell widths from the data of Krause *et al.*[11] by using the value $\Gamma_{L_1}=5.5$ eV determined in the preceding paragraph and the theoretical L_2 and L_3 widths.[4] The calculated M_1, M_4, and M_5 widths are then in good agreement with experiment. The experimental N_1 widths are lower than the calculated value by 1.9 and 1.2 eV but Krause *et al.*[11] indicate the measured L_2N_1 and L_3N_1 widths can be in error by 1 eV. There appears to be a significant discrepancy in the M_2 and M_3 widths. The width of a $3p$ hole at $Z=40$ is dominated by $3p$-$(3d)(4p)$ transitions with emission of an Auger electron at about 100 eV. An error of 10–15 eV in the estimated Auger electron energy should not

TABLE IV. Comparison of calculated and derived level widths for zirconium and silver.

	$Z=40$		$Z=47$	
Level	Meas. (eV)	Calc. (eV)	Meas. (eV)	Calc. (eV)
L_1	5.5	7.3	2.8(5.3)	2.8
L_2	1.8	1.8	2.2	2.6
L_3	1.5	1.5	2.0	2.1
M_1	6.9, 6.2	6.5	8.6, 8.7	9.6
M_2	0.4	2.4	3.1(0.6)	3.7
M_3	0.0	2.4	3.8(1.3)	3.9
M_4	0.2	0.07	0.2, 0.7, 0.2	0.44
M_5	0.2	0.07	0.34	0.44
N_1	4.5, 5.2	6.4	6.6	(42)
N_2	...	...	8.2(5.7)	9.7
N_3	...	...	7.4(4.9)	9.7
N_4	...	...	1.8	0.0
N_5	...	...	1.7	0.0

significantly change the calculated width. Krause *et al.* estimate the error in the L_1-M_2 and L_1-M_3 width as 0.6 eV, which cannot account for the difference between calculated and experimental M_2 and M_3 widths. A possible explanation could be the choice of $\Gamma_{L_1}=5.5$ eV. For the silver data there are two possible sets of level widths depending on the choice of Γ_{L_1}. Parratt uses 5.3 eV, which leads to the values in parenthesis in Table IV. We have argued elsewhere[33] that the correct value should be $\Gamma_{L_1}=2.8$ eV. Using this value in place of Parratt's choice we have the experimental values used in the table. The calculated and measured widths are in excellent agreement except for the N_1 and $N_{4,5}$. The 1.7–1.8-eV width for the N_4 and N_5 levels obtained from the measurements indicates a narrow ($4d$) band rather than a sharp $4d$ level. The discrepancy between calculated and measured $4s$ widths is due to the choice of Auger electron energy. In Fig. 2 we show the Auger electron energy and calculated $4s$ widths for three different energy estimates.[23] Energy estimate (3) uses the expression of Asaad and Burhop[37] and should be the most reliable. However, the ionization thresholds used were taken from the ESCA tabulation[28] and do not include a work-function correction. Such a correction would lower ϵ_3 by 4–5 eV so that ϵ_3 is close to ϵ_2 and the width Γ_{N_1} is in the 6–8-eV region. Widths calculated using energy estimate (2) are shown in parenthesis in Table I. Figure 2 indicates the enormous change in Γ_{N_1} with Auger electron energy. Consequently the widths of the L_2-N_1 and L_3-N_1 lines should be a useful monitor in these materials of $4d$ electron energy shifts relative to core levels.

b. $50< Z \leq 57$. For $Z=54$ and 57 the calculations indicate relatively small widths. That is, the ($4s$)-($4p$)($4d$) and ($4p$)-($4d$)^2 super-Coster-Kronig-transitions are forbidden. This is probably not entirely correct. At $Z=50$ the calculated N_2 and N_3 widths are large, and at $Z=54$ they are a factor of 10 smaller. Thus one expects that between two intermediate Z values there will be a narrowing of the N_2 and N_3 widths. In fact the effect of this is clearly seen in the Xe $4p$ photoelectron spectrum,[38] where one sees a narrow N_3 line and a broad weak structure where the N_2 line should be. However, the ESCA binding-energy tabulation[28] lists the N_3 value for both N_2 and N_3 levels. The calculations were done with the listed energy values, and consequently we made no estimate of the N_2 width. One is led to the question: If the width of the Xe N_2 is large and the N_3 small, how will this affect the Auger spectrum? We discuss this elsewhere.[10]

c. Rare earths, $58 \leq Z \leq 70$. Recent measurements on the $4d$ photoabsorption cross section[39] has stimulated calculations[40-42] on the spectra of inner-shell excitations of the rare earths. At the same time the rare earths have been examined for multiplet splitting due to the high-spin values attainable with a partially filled $4f$ shell.[13,22] Characteristically, if the width of an inner-shell vacancy is dominated by Auger transitions involving electrons from a partially filled shell, and if mul-

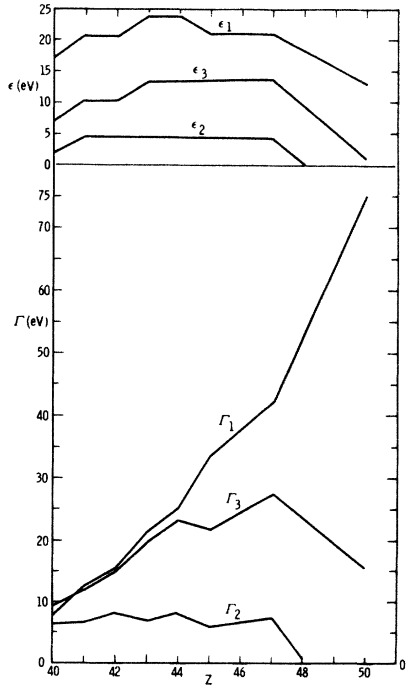

FIG. 2. Calculated $4s$ level widths for $40 \leq Z \leq 50$ for three choices of Auger electron energy in the ($4s$)-($4p$)($4d$) super-Coster-Kronig-process. Also shown are the Auger electron energies.

TABLE V. Comparison of calculated and measured $L_{2,3}$-$M_{4,5}$ line widths for $58 \leq Z \leq 71$. The experimental data is from Ref. 13. The value in parenthesis at $Z = 70$ is obtained by excluding the N_4-$N_5N_{6,7}$ super-Coster-Kronig-process.

	$\Gamma(L_3$-$M_5)$		$\Gamma(L_3$-$M_4)$		$\Gamma(L_2$-$M_4)$		$\Gamma(L_3$-$N_5)$		$\Gamma(L_2$-$N_4)$	
Z	Expt.	Theor.	Expt.	Theor.	Expt.	Theor.	Expt.	Theor.	Expt.	Theor.
58	5.6	3.9	5.2	3.9	5.7	4.6	5.9	3.4	5.8	4.1
60	5.5	4.4	5.5	4.8	7.8	5.5	6.9	4.3	7.2	5.0
63	7.0	4.6	6.5	5.4	8.8	6.2	7.8	5.6	10.2	6.4
65	7.9	5.0	7.7	5.9	7.5	6.8	8.3	7.0	11.0	7.9
67	9.7	5.3	7.3	6.3	7.8	7.2	9.4	8.2	20.1	9.3
70	9.1	5.8	7.2	7.3	7.7	8.4	14.6	11.4	17.3	14.7(12.5)
71	6.2	5.8	5.8	7.3	7.2	8.4	10.2	11.4		

tiplets are formed by adding the quantum number of an inner-shell vacancy to those of the partially filled shell, then the widths of the multiplet components will differ and will depend on the initial term value of the partially filled shell.[23] In general, this leads to a complex calculation. The widths listed in Tables I–III neglect multiplet effects. Demekhin, Platkov, and Lyubivaya[13] examined the $L_{2,3}$-$M_{4,5}$ and $L_{2,3}$-$N_{4,5}$ x-ray emission spectra of the rare earths to see if these emission lines were broadened due to multiplet structure in the final state. They estimate that M_4 and M_5 multiplets can lead to broadening by a few eV, and N_4 and N_5 multiplets to broadening by as much as 10 eV. In Table V we compare the measured linewidths of Ref. 13, with those calculated from Table III and Refs. 4 and 7. The results listed in Table V tend to support the hypothesis of additional broadening due to multiplet splitting in the final state. At $Z = 70$ our calculations include the N_4-$N_5N_{6,7}$ transition; the calculated width with the N_4-$N_5N_{6,7}$ transition omitted is listed in parenthesis. Thus, it appears one cannot determine experimental $M_{2,3}$, $M_{4,5}$, $N_{2,3}$, or $N_{4,5}$ level widths for the rare earths without properly correcting for multiplet splitting. The situation should be simpler for the M_1 and N_1 levels as multiplet splitting leads to a doublet only. In Ref. 23 we show that the calculation of the widths of the M_1 doublets in the iron group transition elements is a complex problem. In Fig. 3 we show the calculated 4s width averaged over the doublet for three different values of Auger energy in the (4s)-(4p)(4f) transition. The major contributions to the 4s widths come from the (4s)-(4p)(4f) transition and the (4s)-(4p)(5p) transition. For these transitions the partial widths are extremely sensitive to Auger electron energy, but the total width is less sensitive.[23] We also show the data of Cohen *et al.*[22] The calculated widths are a factor of 1.5–3.0 larger than the measurements. Fadley and Shirley[43] have also examined the rare-earth photoelectron spectrum, specifically the 4d photoelectrons. At $Z = 54$, Fadley and Shirley[43] measure a 4d width of 1.07 eV, which is consistent with a narrow 4d width and 1.0-eV resolution for their apparatus. At $Z = 63$ they measure a 4d width of 3.8 eV. We calculate a width of 2.1 eV and can attribute a 1.7-eV broadening to multiplet splitting of the N_4 and N_5. This is consistent with the difference between the calculated and measured L_3-N_5 width in Table V, but is considerably smaller than L_2-N_4 width difference. However, at $Z = 70$ and 71 Fadley and Shirley[43] measure 4d widths of 5.4 and 4.2 eV, respectively, while we calculate a width of 7.2 eV. Thus

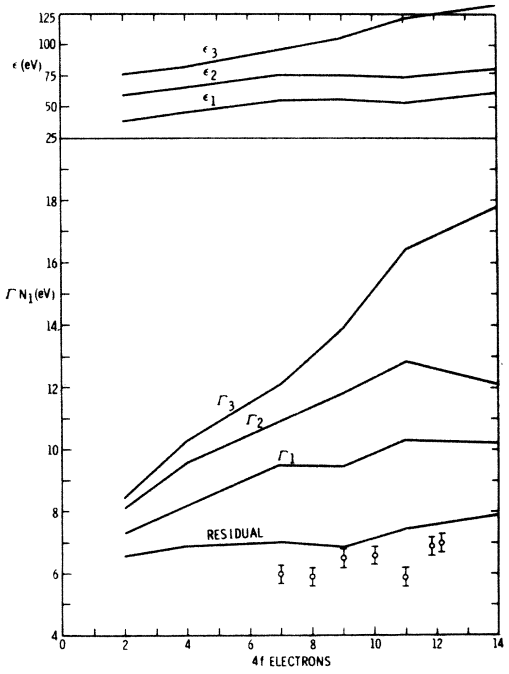

FIG. 3. Calculated 4f level widths for $58 \leq Z \leq 70$ as a function of number of 4f electrons in the (4s)-(4p)(4f) super-Coster-Kronig-transition for three choices of Auger electron energy. The experimental points are from Ref. 22. The line called residual are our calculated widths neglecting the (4s)-(4p)(4f) transition.

near $Z=70$ our calculated $4d$ width is 50% higher than the measured value. The $4d$ widths for $65 \leq Z \leq 79$ are dominated by $4d$-$(4f)^2$ super-Coster-Kronig-transitions. If instead of the energy estimate in Eq. (2), we use the procedure of Asaad and Burhop[37] to find an alternate energy estimate we have for the Auger electron energy ϵ:

$$\epsilon = E(4d) - 2E(4f) + I(4f, 4f),$$

where $E(nl)$ is the binding energy and $I(nl, nl)$ is the interaction energy of a pair of nl electrons.[44] Using Mann's tables[45] to evaluate $I(4f, 4f)$ we found that the above energy estimate was 25% lower than Eq. (2) for $60 \leq Z \leq 70$, and within 10% for $73 \leq Z \leq 79$. In each instance the Auger electron energy was about or greater than 100 eV. Thus, for $60 \leq Z \leq 83$, it appears that the difference between experimental and calculated $4d$ widths cannot be attributed to the sensitivity to energy estimate in the $4d$-$(4f)^2$ Auger transition rate.

d. $Z \geq 70$. In Table VI we list the L-M and L-N widths measured by Richtmyer, Barnes, and Ramberg for gold,[15] and determine the level widths by using 5.2 eV for the L_3 width. This is the value calculated by the author.[4] Chen, Crasemann, and Kostroun,[5] and Walters and Bhalla[6] calculate an L_3 width of 5.7 eV at $Z=80$, so that at $Z=79$ three calculated L_3 widths are within 10% of one another. Richtmyer, Barnes, and Ramberg[15] also determine M and N level widths, but they use an L_3 width of 4.4 eV obtained from an analysis of the L_3 threshold photoabsorption cross section. From threshold photoabsorption they find the L_2 width is 1.4 eV greater than the L_3 width. However, they disregard this, as the analysis of the x-ray emission widths leads to an L_2 width 0.7 eV smaller than the L_3 width! Our calculations indicate an L_2 width 1.6 eV greater than the L_3 width for gold. Thus there appears to be a basic difficulty in determining linewidths in x-ray emission spectra. Neglecting this point, we find the experimental level widths in the fourth column of Table VI. The data of Ref. 15 lead to an M_2 width smaller than the M_3 width by 1.4 eV. Cooper,[14] whose results we discuss later, finds the situation reversed with the M_2 width larger than the M_3 width by 2.5 eV. Thus for the M shell of gold it appears the calculated and experimental values are in reasonable agreement. For the N shell, however, the calculated widths are a factor of 1.3–2.0 larger than the measured values. For the N_4 and N_5 the difference between calculated and experimental widths is almost identical to the difference seen in comparing the calculated width with electron photoemission data[43] at $Z=70$. Cooper[14] made systematic measurements of selected linewidths in the $70 \leq Z \leq 81$ range. Cooper's measurements do not permit a direct evaluation of the L_2-L_3 level width difference. However, as his experiment was performed at a comparable wavelength and with the same apparatus as Richtmyer, Barnes, and Ramberg,[15] for purposes of analysis we assume his measured L_2-L_3 width difference would be zero or negative. As a result we used the computed L_3 width for both

TABLE VI. Comparison of calculated and derived level widths for gold.

Transition	Width (eV)	Level	Width (eV) Expt. (Ref. 15)	Width (eV) Expt. (Ref. 14)	Width (eV) Calc.
L_1-M_2	19.4	L_1[a]	9.8, 9.2		
L_1-M_3	20.8	L_2[b]	4.7, 4.5, 4.0, 5.0		6.8
L_1-M_4	13.1	L_3	5.2[c]		5.2
L_1-M_5	12.1	M_1	14.6[d]		20.9
L_1-N_2	17.2	M_2	9.9[e]	11.4	14.7
L_1-N_3	15.2	M_3	11.3[e]	8.9	9.7
L_2-M_1	19.3	M_4	3.3[b]	2.2	2.8
L_2-M_4	7.8	M_5	2.9[b]		2.7
L_2-N_1	15.1	N_1	11.1[b]		15.9
L_2-N_4	10.8	N_2	7.7[e]	8.3	14.2
L_3-M_1	19.8	N_3	5.7[e]	6.6	12.9
L_3-M_4	8.5	N_4	5.8[b]	4.9	8.8
L_3-M_5	8.1	N_5	5.1[b]	4.9	8.4
L_3-N_1	16.3				
L_3-N_4	11.0				
L_3-N_5	10.3				

[a] Obtained using widths found by using footnote d.
[b] Obtained using M_4 and M_5 widths found by using footnote d.
[c] We use the calculated L_3 width.
[d] Obtained using $\Gamma_{L_3} = 5.2$.
[e] Obtained using $\Gamma_1 = 9.5$ eV from footnote b.

TABLE VII. Comparison of calculated and derived level widths for $70 \leq Z \leq 79$. Also shown are measured and calculated M-N line widths for tungsten.

Level \ Z	Level width (eV)					
	70	73	74	76	77	79
L_1	5.4	5.7	5.8	6.0	6.4	7.2
L_2	4.2	4.6	4.7	4.8	5.0	5.2
	4.2	4.6	4.7	4.8	5.0	5.2
L_3	4.2	4.6	4.7	4.8	5.0	5.2
	4.2	4.6	4.7	4.8	5.0	5.2
M_2	8.5	8.4	9.3	11.1	11.3	11.4
	11.8	12.0	12.3	13.9	14.2	14.7
M_3	7.5	7.0	6.5	8.7	8.5	8.9
	11.6	10.8	10.4	9.3	9.3	9.4
M_4	3.2	2.0	1.8	1.7	1.8	2.2
	3.1	3.3	3.6	4.2	3.7	2.8
N_2		5.9	6.3	8.0	8.2	8.3
		14.6	13.8	14.0	14.5	14.2
N_3	4.8	4.5	5.2	6.6	6.9	6.6
	12.1	12.9	12.3	12.5	12.8	12.9
N_4		4.9	4.6	4.5	4.6	4.9
		7.7	7.9	8.1	8.6	8.8
N_5		5.2	5.1	5.0	4.7	4.9
		7.6	7.7	7.9	8.3	8.4

Line	Line Widths (eV) at $Z = 74$ Width (Ref. 18)	Width (Ref. 14)	Calc.
M_5-N_6	0.3		1.9
M_5-N_7	1.7		1.9
M_4-N_6	2.1	1.8	3.6
M_4-N_3	0.8	7.0	15.9
M_5-N_3	12.5		14.2
M_4-N_2	2.3	8.1	17.4

the L_2 and L_3 widths. The theoretical L_3 widths[4-6] are in good agreement in this range. For the L_1 width we used an eyeball fit to the experimental values tabulated in this range.[32] The theoretical estimates[4,5] of L_1 widths near $Z = 79$ are uncertain because it is not clear if the L_1-L_3M_4 and L_1-L_3M_5 transitions are allowed or forbidden. Using these L-shell widths we obtain the M- and N-subshell widths listed in Table VII, where the first entry is the value derived from the measured linewidth and the second is the calculated value. As in the comparison with the measurements on gold, the calculated M-shell widths are in reasonable agreement with experiment, while for the N shell the calculated widths are a factor of 1.5–2.5 larger than the measured values. Cooper's $4d$ widths are consistent with the measurements from photoelectron spectroscopy.[43] Munier, Bearden, and Shaw[18] have measured the width of various M-N lines in tungsten. The lines and their widths are listed in

TABLE VIII. Comparison of derived and calculated level widths for uranium. The experimental values are from Ref. 17.

Line	Measured width (eV)	Level	Measured width (eV)	Calc.
L_1-M_2	32.2	M_2	12.9	20.2
L_1-M_3	18.8	M_4	−0.5	12.6
L_1-N_2	39.4	N_2	20.1	7.5
L_2-M_4	14.3	M_4	3.4, 2.2	4.5
L_2-N_1	32.4	N_1	21.5, 20.3	11.8
L_2-N_4	16.0	N_4	5.1, 3.9	4.2
L_3-M_4	14.4	M_4	7.1	4.5
L_3-M_5	13.1	M_5	5.8	4.2
L_3-N_1	19.4	N_1	12.1	11.8
L_3-N_5	16.1	N_5	8.8	4.2

the second-half of Table VII. We also list calculated linewidths from Cooper's measurements (the first-half of Table VII) and our calculated linewidths. The measured M_4-N_2 and M_4-N_3 widths are at least a factor of 4 smaller than either calculation, while the measured M_5-N_3 linewidth implies an N_3 level width of about 10 eV. Clearly the results of Munier, Bearden, and Shaw[18] are puzzling and indicate serious difficulty in interpreting linewidths in x-ray emission spectroscopy. We have seen that there is an inconsistency in gold between the L_2-L_3 level width difference found by x-ray emission spectroscopy and by threshold photoionization.

Williams[17] has measured the widths of various L-M and L-N lines in uranium. In Table VIII we list the measured linewidths, and level widths obtained using L-shell widths calculated by the author[46] ($\Gamma_{L_1} = 19.3$ eV, $\Gamma_{L_2} = 10.9$ and 12.1 eV, and $\Gamma_{L_3} = 7.3$ eV). Two entries are given for Γ_{L_2} because while the L_2-L_3M_4 transition appears forbidden in uranium using Eq. (2), it was found necessary[46] to include the L_2-L_3M_4 transition to bring the calculated $f_{2,3}$ value into reasonable agreement with experiment. With the exception of the N_5 level the level widths derived from transitions involving L_3 are in good agreement with experiment. The M_4 and N_4 widths derived using the calculated L_2 widths are in reasonable agreement with experiment, while the calculated N_1 level width, which is in excellent agreement with the value obtained from the L_3-N_1 linewidth, is only one-half the value obtained from the L_2-N_1 linewidth. There appears no way to reconcile the calculated M_2, M_3, and N_2 level widths with the measured L_1 linewidths. If Γ_{L_1} were 9.3 rather than 19.3, the computed and derived M_2 and M_3 widths would then be in reasonable agreement. However, the derived N_2 width would then be 30 eV, while the calculated value is 7.5 eV. Thus, again we find anomalies in

TABLE IX. Auger transition rates for initial f holes.

Initial Electrons	Transition rate (Per a.t.u.)
s,s'	$2\pi\times 2\tau^2[D(3,3)^2+E(3,3)^2-D(3,3)E(3,3)]$
s,p	$2\pi\times\frac{6}{7}\{3[D(3,2)^2+E(2,2)^2-D(3,2)E(2,2)]+4[D(3,4)^2+E(4,4)^2-D(3,4)E(4,4)]\}$
s,d	$2\pi\{\frac{18}{7}[D(3,1)^2+E(1,1)^2-D(3,1)E(1,1)]+\frac{8}{3}[D(3,3)^2+E(3,3)^2-D(3,3)E(3,3)]$ $+\frac{100}{21}[D(3,5)^2+E(5,5)^2-D(3,5)E(5,5)]\}$
s,f	$2\pi\{2[D(3,0)^2+E(0,0)^2-D(3,0)E(0,0)]+\frac{8}{3}[D(3,2)^2+E(2,2)^2-D(3,2)E(2,2)]$ $+\frac{36}{11}[D(3,4)^2+E(4,4)^2-D(3,4)E(4,4)]+\frac{200}{33}[D(3,6)^2+E(6,6)^2-D(3,6)E(6,6)]\}$
p,p'	$2\pi\times 18\tau^2\{\frac{6}{35}[D(2,1)^2+E(2,1)^2-D(2,1)E(2,1)]+\frac{9}{35}[D(2,3)^2+E(2,3)^2-\frac{1}{21}D(2,3)E(2,3)]$ $+\frac{16}{63}[D(4,3)^2+E(4,3)^2-\frac{1}{28}D(4,3)E(4,3)]+\frac{20}{63}[D(4,5)^2+E(4,5)^2-D(4,5)E(4,5)]$ $-\frac{12}{49}[D(2,3)E(4,3)+D(4,3)E(2,3)]\}$
p,d	$2\pi\times 30\{\frac{3}{35}[D(2,0)^2+E(1,0)^2-D(2,0)E(1,0)]+\frac{6}{245}[7E(1,2)^2+5D(2,2)^2-D(2,2)E(1,2)]$ $+\frac{4}{245}[7E(3,2)^2+10D(4,2)^2-D(4,2)E(3,2)]-\frac{12}{245}[2D(2,2)E(3,2)+3E(1,2)D(4,2)]$ $+\frac{2}{735}[81D(2,4)^2+56E(3,4)^2-6D(2,4)E(3,4)]-\frac{10}{49}[D(2,4)E(5,4)+\frac{2}{3}D(4,4)E(3,4)]$ $+[10/(77\times 63)][72D(4,4)^2+105E(5,4)^2-2D(4,4)E(5,4)]+\frac{20}{77}[D(4,6)^2+E(5,6)^2-D(4,6)(E(5,6)]\}$
p,f	$2\pi\times 42\{\frac{27}{245}D(2,1)^2+\frac{4}{35}D(2,3)^2+\frac{10}{49}D(2,5)^2+\frac{16}{147}D(4,1)^2$ $+\frac{8}{77}D(4,3)^2+[80/(13\times 49)]D(4,5)^2+\frac{100}{429}D(4,7)^2+\frac{1}{7}E(0,1)^2$ $+\frac{8}{105}E(2,1)^2+\frac{4}{35}E(2,3)^2+\frac{8}{77}E(4,3)^2+\frac{10}{77}E(4,5)^2$ $+[200/(13\times 77)]E(6,5)^2+[100/(13\times 33)]E(6,7)^2-\frac{3}{49}D(2,1)E(0,1)$ $-\frac{12}{245}D(2,1)E(2,1)-\frac{8}{245}D(2,3)E(2,3)-\frac{4}{49}D(2,3)E(4,3)$ $-[100/(11\times 49)]D(2,5)E(4,5)-[100/(11\times 49)]D(2,5)E(6,5)-\frac{4}{49}D(4,1)E(0,1)$ $-\frac{4}{147}D(4,1)E(2,1)-\frac{4}{49}D(4,3)E(2,3)-[12/(11\times 49)]D(4,3)E(4,3)$ $-[60/(11\times 49)]D(4,5)E(4,5)-[100/(49\times 143)]D(4,5)E(6,5)-[100/(11\times 39)]D(4,7)E(6,7)\}$
d,d'	$2\pi\times 50\tau^2\{\frac{18}{175}[D(1,1)^2+E(1,1)^2-\frac{3}{5}D(1,1)E(1,1)]+(12/175)[D(3,1)^2$ $+E(3,1)^2-\frac{2}{5}D(3,1)E(3,1)]-\frac{36}{875}[D(1,1)E(3,1)+D(3,1)E(1,1)]$ $+\frac{27}{175}[D(1,3)^2+E(1,3)^2-\frac{1}{35}D(1,3)E(1,3)]+\frac{16}{225}[D(3,3)^2+E(3,3)^2$ $-\frac{19}{60}D(3,3)E(3,3)]+[100/(21\times 33)][D(5,3)^2+E(5,3)^2-\frac{1}{210}D(5,3)E(5,3)]$ $-\frac{24}{875}[D(1,3)E(3,3)+D(3,3)E(1,3)]-\frac{6}{49}[D(1,3)E(5,3)+D(5,3)E(1,3)]$ $-\frac{4}{189}[D(3,3)E(5,3)+D(5,3)E(3,3)]+\frac{8}{63}[D(3,5)^2+E(3,5)^2-\frac{1}{6}D(3,5)E(3,5)]$ $+[100/(13\times 63)][D(5,5)^2+E(5,5)^2-\frac{2}{15}D(5,5)E(5,5)]-\frac{20}{189}[D(3,5)E(5,5)+D(5,5)E(3,5)]$ $+\frac{30}{143}[D(5,7)^2+E(5,7)^2-D(5,7)E(5,7)]\}$
d,f	$2\pi\times 70\{\frac{1}{35}[\frac{27}{7}D(1,2)^2+\frac{36}{7}D(1,4)^2+\frac{4}{3}D(3,0)^2+\frac{16}{9}D(3,2)^2+\frac{24}{11}D(3,4)^2]$ $+\frac{10}{33}[\frac{8}{21}D(3,6)^2+\frac{50}{147}D(5,2)^2+\frac{180}{637}D(5,4)^2+\frac{1}{3}D(5,6)^2+\frac{8}{13}D(5,8)^2]$ $+\frac{1}{7}[E(0,2)^2+\frac{4}{15}E(2,0)^2+\frac{8}{21}E(2,2)^2+\frac{24}{35}E(2,4)^2+\frac{36}{77}E(4,2)^2]$ $+\frac{10}{77}[\frac{36}{77}E(4,4)^2+\frac{9}{11}E(4,6)^2+\frac{150}{143}E(6,4)^2+\frac{28}{33}E(6,6)^2+\frac{56}{39}E(6,8)^2]$ $-[9/(35\times 49)]D(1,2)[7E(0,2)+8E(2,2)+6E(4,2)]-\frac{4}{105}D(3,0)E(2,0)$ $-[12/(11\times 35\times 49)]D(1,4)[11E(2,4)+45E(4,4)+175E(6,4)]-[20/(63\times 121)]D(3,6)[9E(4,6)+35E(6,6)]$ $-[4/(21\times 105)]D(3,2)[21E(0,2)-11E(2,2)+18E(4,2)]-[10/(9\times 121)]D(5,6)[9E(4,6)+2E(6,6)]$ $-[4/(121\times 245)]D(3,4)[242E(2,4)+45E(4,4)+175E(6,4)]-\frac{10}{147}D(5,2)[E(0,2)+\frac{10}{3}E(2,2)+\frac{3}{11}E(4,2)]$ $-[80/(13\times 33)]D(5,8)E(6,8)-\frac{20}{343}D(5,4)[E(2,4)+\frac{54}{121}E(4,4)+\frac{35}{1573}E(6,4)]\}$

TABLE IX. *(Continued)*

Initial Electrons	Transition rate (Per a.t.u.)
$f\,f'$	$2\pi\times 987^2\{\frac{1}{7}[D(0,3)^2+E(0,3)^2-\frac{1}{7}D(0,3)E(0,3)]$
	$+\frac{12}{245}[D(2,1)^2+E(2,1)^2-\frac{2}{7}D(2,1)E(2,1)]+\frac{16}{315}[D(2,3)^2+E(2,3)^2-\frac{19}{84}D(2,3)E(2,3)]$
	$+\frac{40}{441}[D(2,5)^2+E(2,5)^2-\frac{5}{42}D(2,5)E(2,5)]+\frac{24}{539}[D(4,1)^2+E(4,1)^2-\frac{3}{14}D(4,1)E(4,1)]$
	$+\frac{36}{847}[D(4,3)^2+E(4,3)^2-\frac{97}{154}D(4,3)E(4,3)]$
	$+[360/(49\times 143)][D(4,5)^2+E(4,5)^2+\frac{23}{154}D(4,5)E(4,5)]$
	$+[150/(13\times 121)][D(4,7)^2+E(4,7)^2-\frac{3}{11}D(4,7)E(4,7)]$
	$+[(100\times 100)/(21\times 39\times 121)][D(6,3)^2+E(6,3)^2-\frac{1}{924}D(6,3)E(6,3)]$
	$+[100/(33\times 39)][D(6,5)^2+E(6,5)^2-\frac{1}{33}D(6,5)E(6,5)]$
	$+[2400/(143\times 187)][D(6,7)^2+E(6,7)^2-\frac{5}{22}D(6,7)E(6,7)]$
	$+[400/(17\times 143)][D(6,9)^2+E(6,9)^2-D(6,9)E(6,9)]$
	$-\frac{4}{147}[D(0,3)E(2,3)+D(2,3)E(0,3)]-\frac{18}{539}[D(0,3)E(4,3)+D(4,3)E(0,3)]$
	$-[100/(49\times 33)][D(0,3)E(6,3)+D(6,3)E(0,3)]-\frac{12}{343}[D(2,1)E(4,1)+D(4,1)E(2,1)]$
	$+\frac{12}{539}[D(2,3)E(4,3)+D(4,3)E(2,3)]-[500/(27\times 539)][D\,2,3)E(6,3)]+D(6,3)E(2,3)]$
	$-[120/(77\times 49)][D(2,5)E(4,5)+D(4,5)E(2,5)]-[100/(33\times 63)][D(2,5)E(6,5)+D(6,5)E(2,5)]$
	$-[300/(121\times 539)][D(4,3)E(6,3)+D(6,3)E(4,3)]-[300/(77\times 143)][D(4,5)E(6,5)+D(6,5)E(4,5)]$
	$-[1200/(121\times 143)][D(4,7)E(6,7)+D(6,7)E(4,7)]\}$

level widths determined from x-ray emission spectroscopy.

V. CONCLUSIONS

For $40 \leq Z \leq 50$ the calculated and measured $4p$ widths are in reasonable agreement if one uses Brewer's[36] model for binding in the solid at $Z=42$, 44, and 45. The $4s$ widths are in agreement with experiment providing a judicious choice is made for the Auger electron energy. Our calculations indicate that for xenon one can account for the nonappearance of an N_2 peak in photoelectron spectroscopy because the N_2 level width is large due to the N_2-$(4d)^2$ transition, while the N_3 level width is relatively narrow as the N_3-$(4d)^2$ transition is energetically forbidden. At the onset of $4f$ electrons with the rare earths we begin to find significant discrepancies between calculated and experimental level widths. To some extent this is due to sensitivity to Auger electron energy of super-Coster-Kronig-transitions involving $4f$ electrons. The discrepancies, however, occur not only in the rare earths, where the $4f$ shell is being filled and Eq. (2) significantly overestimates the Auger electron energy, but also the discrepancy persists up to gold ($Z=79$). The energy estimate of Eq. (2) is in reasonable agreement with a more accurate estimate for $70 \leq Z \leq 79$. Thus we do not attribute all the discrepancy to the energy sensitivity of the Auger transition rate. Most of the comparisons of calculated and experimental level widths used linewidths measured in x-ray emission spectroscopy. Systematic comparison of such linewidths indicated discrepancies between experiments in different spectral regions, and discrepancies between level widths measured with different techniques. However, at $Z=70$, the $4d$ width measured by x-ray spectroscopy was in good agreement with the $4d$ width measured by photoelectron spectroscopy. Extensive measurements of photoelectron widths for the N shell should be performed. Auger transitions are the dominant decay mechanism for N-shell holes, and the fluorescence yields in Tables I–III can be multiplied by a factor $\Gamma_{\text{calc}}/\Gamma_{\text{TRUE}}$ to find improved N-shell fluorescence-yield values.

APPENDIX

The Auger transition rates for an initial f hole are written in terms of direct and exchange integrals $D(K, l_2)$ and $E(K, l_2)$, where

$$D(K,l_2)=\frac{1}{2K+1}\int_0^\infty\int_0^\infty R_{nf}(r_1)R_{\epsilon,l_2}(r_2)\frac{(r_<)^K}{(r_>)^{K+1}}\times R_{n_3,l_3}(r_1)R_{n_4,l_4}(r_2)r_1^2r_2^2\,dr_1\,dr_2\,,$$

where $R_{n,l}(r)$ is a one-electron eigenfunction and ϵ is the energy of the electron in the continuum. $E(K, l_2)$ is obtained by interchanging n_3, l_3 and n_4, l_4

in the above expression for $D(K, l_2)$. When the continuum electron is normalized to one per Hartree (27.2 eV) and r is in units of Bohr radii the Auger transition rate is per atomic time unit (1 a.t.u. $=2.42\times10^{-17}$ sec). The factor τ^2 is $\frac{1}{2}$ if l_3 and l_4 are equivalent electrons, and unity otherwise. The transition rate expressions for various l_3 and l_4 are listed in Table IX.

---

*This work was supported by the U. S. Atomic Energy Commission.

[1]E. J. McGuire, Phys. Rev. A 2, 273 (1970).
[2]V. O. Kostroun, M. H. Chen, and B. Crasemann, Phys. Rev. A 3, 533 (1971).
[3]D. L. Walters and C. P. Bhalla, Phys. Rev. A 3, 1919 (1971).
[4]E. J. McGuire, Phys. Rev. A 3, 587 (1971).
[5]B. Crasemann, M. H. Chen, and V. O. Kostroun, Phys. Rev. A 4, 1 (1971); Phys. Rev. A 4, 2161 (1971).
[6]D. L. Walters and C. P. Bhalla, Phys. Rev. A 4, 2164 (1971).
[7]E. J. McGuire, Phys. Rev. A 5, 1043 (1972).
[8]C. P. Bhalla, Phys. Rev. A 6, 1409 (1972).
[9]L. O. Werme, T. Bergmark, and K. Siegbahn, Phys. Scr. 6, 141 (1972).
[10]E. J. McGuire (unpublished).
[11]M. O. Krause, F. Wuillemier, and C. W. Nestor, Jr., Phys. Rev. A 6, 871 (1972).
[12]L. G. Parratt, Phys. Rev. 54, 99 (1938).
[13]V. F. Demekhin, A. I. Platkov, and M. V. Lyubivaya, Zh. Eksp. Teor. Fiz 62, 49 (1972) [Sov. Phys.—JETP 35, 28 (1972)].
[14]J. N. Cooper, Phys. Rev. 61, 234 (1942).
[15]F. K. Richtmyer, S. W. Barnes, and E. Ramberg, Phys. Rev. 46, 843 (1934).
[16]S. K. Allison, Phys. Rev. 34, 176 (1929).
[17]J. H. Williams, Phys. Rev. 37, 1431 (1931).
[18]J. H. Munier, J. A. Bearden, and C. H. Shaw, Phys. Rev. 58, 537 (1940).
[19]A. P. Lukirskii and T. M. Zimkina, Izv. Akad. Nauk. SSSR Ser. Fiz. 27, 330 (1963) [Bull. Acad. Sci. USSR 27, 339 (1963)].
[20]G. Dannhäuser and G. Wiech, Phys. Lett. A 35, 208 (1971).
[21]M. O. Krause, Chem. Phys. Lett. 10, 65 (1971).
[22]R. L. Cohen, G. K. Wertheim, A. Rosencwaig, and H. J. Guggenheim, Phys. Rev. B 5, 1037 (1972).
[23]E. J. McGuire (unpublished).
[24]E. J. McGuire, Nucl. Phys. A 172, 127 (1971).
[25]W. Mehlhorn (private communication).
[26]W. N. Asaad, Nucl. Phys. 44, 415 (1963).
[27]V. S. Red'Kin, V. V. Zashkvara, M. I. Karsunskii, and E. V. Tsveiman, Fiz. Tverd. Tela 13, 1511 (1971) [Sov. Phys.—Solid State 13, 1269 (1971)].
[28]K. Siegbahn *et al.*, in *ESCA, Atomic, Molecular and Solida State Structure Studied by Means of Electron Spectroscopy* (Nova Acta Regiae Societatis Upsaliensis, Uppsala, 1967), Ser. IV, Vol. 20.
[29]F. Herman and S. Skillman, *Atomic Structure Calculations* (Prentice-Hall, Englewood Cliffs, N.J., 1963).
[30]A complete set of model parameters, matrix elements, and transition rates are available from the author [E. J. McGuire, Sandia Report No. RS 5211/001 (unpublished)].
[31]M. Siegbahn and T. Magnusson, Z. Phys. 88, 559 (1934).
[32]B. Ekstig and E. Källne, cited by K. Sevier [Low Energy Electron Spectrometry (Wiley-Interscience, New York (1972)].
[33]E. J. McGuire, Phys. Rev. A 5, 2313 (1972).
[34]C. E. Moore, *Atomic Energy Levels*, NBS Circular No. 467 (U. S. GPO, Washington, D. C., 1957).
[35]B. Ekstig, E. Källne, E. Noreland, and R. Manne, Phys. Scr. 2, 38 (1970).
[36]L. Brewer, Science 161, 115 (1968).
[37]W. N. Asaad and E. H. S. Burhop, Proc. Phys. Soc. (Lond.), 71, 369 (1958).
[38]K. Siegbahn *et al.*, *ESCA Applied to Free Molecules* (Elsevier, New York, 1969).
[39]T. M. Zimkina, V. A. Fomichev, S. A. Gribovskii, and I. I. Zhukova, Fiz. Tverd. Tela 9, 1447 (1967) [Sov. Phys.—Solid State 9, 1128 (1967)].
[40]A. F. Starace, Phys. Rev. B 5, 1773 (1972).
[41]J. Sugar, Phys. Rev. B 5, 1785 (1972).
[42]J. L. Dehmer and A. F. Starace, Phys. Rev. B 5, 1792 (1972).
[43]C. S. Fadley and D. A. Shirley, Phys. Rev. A 2, 1109 (1970).
[44]J. C. Slater, *Quantum Theory of Atomic Structure* (McGraw-Hill, New York, 1960), Vol. I.
[45]J. B. Mann, Los Alamos Scientific Laboratory Report No. LASL-3690, 1967 (unpublished).
[46]E. J. McGuire, U. S. Atomic Energy Commission Report No. CONF-720404, 1973 (unpublished).